ELSEVIER

Chemical Engineering Journal 137 (2008) 436–442

Chemical Engineering Journal

www.elsevier.com/locate/cej

Synthesis and characterization of acid-activated Serbian smectite clays obtained by statistically designed experiments

Tatjana Novaković [a,*], Ljiljana Rožić [a], Srđan Petrović [a], Aleksandra Rosić [b]

[a] *IChTM-Department of Catalysis and Chemical Engineering, Njegoševa 12, Belgrade, Serbia*
[b] *Faculty of Mining and Geology, University of Belgrade, Đušina 7, Belgrade, Serbia*

Received 9 February 2007; received in revised form 18 May 2007; accepted 2 June 2007

Abstract

Statistically designed experiments were done to study the recovery of Mg content from natural smectite clays from Serbia by hydrochloric acid leaching. The effects of relevant factors, such as temperature, leaching time, acid normality, solid-to-liquid ratio and stirring rate on leaching yield of MgO have been investigated. Experiments have been planned by the factorial design method. To test the significance of the effects, an analysis of variance has been conducted at 95% confidence intervals.

The structural and adsorption properties of the starting smectite clay and the sample activated at chosen conditions were investigated by means of a model. Scanning electron microscopy (SEM) and nitrogen adsorption–desorption were used to analyze the morphological characteristic of the starting and the activated sample. The results from the nitrogen adsorption–desorption isotherms show that the activated smectite clay possess a narrow pore size distribution of about 2 nm, and a large specific surface area of 238 m^2/g. The results of X-ray diffraction (XRD) and infrared analysis (IR) of starting and activated samples confirmed that smectite was the dominant mineral phase. Besides, chemical treatment of smectite clay with HCl produces an adsorbent with optimal porosity and other adsorption properties suitable for many industrial processes.

Keywords: Factorial design; Acid-activated smectite clay; Mesoporous adsorbent

1. Introduction

Physical, chemical and adsorption properties of natural adsorbents depend on the crystal structure of their constituent clay minerals [1]. Adsorption properties of adsorbents based on bentonite are a function of the content of montmorillonite and the nature and the number of interlayer cations. In order to remove impurities and various exchangeable cations from smectite and produce a homogeneous and well-defined material for use as adsorbent and catalyst, different treatments have been used, most frequently with inorganic acids [2,3]. Important physical changes in acid-activated smectite are the increase of the specific surface area and of the average pore volume, depending on acid strength, time and temperature of treatment [4–10]. A large increase of the pore volume and a broadening of the pore size distribution in the range of pore radius 0.7–3.0 nm in acid-activated smectite indicate that higher acid concentrations cause structural changes and partial decomposition of montmorillonite [11].

Activation proceeds with partial dissolution of smectite, described by pseudo first-order kinetics [12,13] and is characterized by an initial replacement of the interlayer cations by H^+ [14], followed by dissolution of the tetrahedral and octahedral sheets and subsequent release of the structural cations [14–17]. Octahedral cations such as Al^{3+}, Fe^{2+}, Fe^{3+}, and Mg^{2+} can be depleted by treating the clay minerals with acids at elevated temperatures with the rates of depletion generally following the order $Mg^{2+} > Fe^{2+} > Fe^{3+} > Al^{3+}$ [9,18,19].

Some studies on the performance of acid-activated clay and the factorial design method in this study were found in the literature [20–24]. Despite numerous studies, no definite relationship exists between the performance of acid-activated clay and the composition or other properties of the original clay. Hence, each clay has to be specifically activated and tested for its performance.

In this study, statistically designed experiments were performed to investigate the leaching yield of MgO from smectitic clay. MgO content was chosen as process response, because

* Corresponding author. Tel.: +381 11 2630 213.
E-mail address: tnovak@nanosys.ihtm.bg.ac.yu (T. Novaković).

1385-8947/$ – see front matter © 2007 Elsevier B.V. All rights reserved.
doi:10.1016/j.cej.2007.06.003

Mg is released more readily then other octahedral cation during activation. The first-order model, which relates the MgO leaching yield to process factors, was obtained [9]. Also, this paper presents the results of the investigation of the changes of textural properties of acid-activated Serbian smectitic clays, depends on five relevant factors, such as temperature, leaching time, acid normality, solid-to-liquid ratio and stirring rate.

2. Experimental

2.1. Materials

Smectite from Bogovina, Serbia, was used as the raw material.

Natural smectite clay (A) with particles size of mostly less than 75 μm (−200 mesh ASTM), dried at 383 K, having the following average composition (% by wt.) SiO_2-69.12, Al_2O_3-14.01, Fe_2O_3-5.43, CaO-1.62, MgO-2.57, Na_2O-1.33, K_2O-0.66, TiO_2-0.57 and loss ignition 4.69 was used as the starting material. The CEC was determined by the standard method using 1 M NH_4Cl and it was 78 meq/100 g.

2.2. Factorial design

Factorial design is widely used in statistical modeling to obtain empirical linear models between the process response and the process factors. In this regard, the experiments were designed to estimate the main effects, as well as the interaction effects, by using a 2^n factorial design where each variable was investigated at two levels, high and low. In the planning and analysis of the experiments, coded values are usually applied instead of the absolute values of the variables. The relationship between a coded value (X) and an absolute value (Z) is as follows:

$$X = \frac{2(Z - Z_o)}{(Z_2 - Z_1)} \quad (1)$$

where Z_1 is the low level, Z_2 the high level, and Z_o is the medium level of the variable [20–22].

2.3. Synthesis

The chemical activation was carried out under atmospheric pressure in a jacketed glass reactor equipped with a reflux condenser, a thermometer and a stirrer. A typical run was carried out as follows: specified amounts of hydrochloric acid of known concentration and smectite clay were loaded into the glass reactor. The stirring speed was held constant by means of a digitally controlled stirrer. At the end of the experiment, the content of the reactor was immediately filtered. The activated clay was washed free of chlorides with a hot water to pH 4.5 and dried at 383 K to a constant weight.

2.4. Characterization

The contents of the metal cations in the natural clay and the content of major octahedral cations, Mg^{2+}, total Fe, Al^{3+}, in the activated samples are determined by induced coupled plasma (ICP Spectroflame M–Spectro). The percentage of cations removed from the smectite after acid activation is shown in Table 1.

Table 1
Quantities of cations removed from smectite by acid treatment, expresed in terms of oxides

Run	Content of oxides (%)		
	MgO	Fe_2O_3	Al_2O_3
1	11.98	1.11	2.19
2	17.23	2.58	5.24
3	32.24	16.02	15.87
4	31.95	14.36	17.99
5	13.44	2.39	5.24
6	19.85	6.63	0.07
7	41.86	29.46	24.57
8	29.03	11.42	11.88
9	39.67	18.97	23.77
10	21.89	6.44	6.51
11	6.88	0.37	0.53
12	0.63	0.92	0.80
13	5.87	0.55	0.93
14	37.93	13.44	14.28
15	30.34	18.42	21.31
16	22.04	22.74	26.49
17	25.24	12.34	9.83
18	25.24	12.34	9.83
19	25.24	12.34	9.83

N_2 adsorption–desorption isotherms were collected on a Sorptomatic 1990 Thermo Finningen surface area and pore size analyzer at 77 K. The surface area was calculated by the BET method and the distribution of the pore diameter was calculated by the procedure given by Lippens et al. [25]. The crystalline phases were identified by X-ray powder diffraction (XRD), Philips PW 1710 with Cu Kα radiation (40 kV, 30 mA, λ = 0.154178 nm). X-ray diffractograms of disoriented powders were obtained for the 2θ angles ranging from 3° to 70°.To identify clay minerals, X-ray diffraction patterns of the oriented slides were also recorded in the range of 3–15° (2θ) on air-dried oriented samples (AD), ethylene glycol vapor saturated samples (EG) and after heating at 723 K. The Greene-Kelley test was also carried out to distinguish montmorillonite from beidellite. Sample was Li-saturated, heated at 473 K and then saturated with ethylene glycol. The infrared (IR) spectra were measured by a Perkin-Elmer 983 G IR-spectrometer in the spectral range 4000–250 cm^{-1}. The KBr pressed disc technique (2 mg of sample and 200 mg of KBr) was used. The morphological characteristic of the samples was investigated by scanning electron microscope JEOL, model JSM 6460-LV at 25 keV.

3. Results and discussion

The most important parameters affecting the efficiency of an adsorbent are reaction temperature, hydrochloric acid normality, stirring speed, solid to liquid ratio and reaction time. In order to study the combined effect of these factors, experiments were

Table 2
Factor levels used in the experiments

Factor	Physical	Low level (−)	Medium level (0)	High level (+)
X_1	Temperature (K)	343	353	363
X_2	HCl concentration (N)	3.0	4.5	6.0
X_3	Stirring speed (rpm)	300	450	600
X_4	Solid/liquid ratio	1:3	1:4	1:6
X_5	Time (h)	1	2	3

performed at different combinations of the physical parameters using statistically designed experiments.

The parameters, such as reaction temperature (X_1), hydrochloric acid normality (X_2), stirring speed (X_3), solid to liquid ratio (X_4) and reaction time (X_5), were chosen as independent variables and their effect on the leaching yield of MgO from the smectite clay from Serbia was investigated in the light of pre-experiments. The factor levels are shown in Table 2.

With five factors, 2^5 full-factorial experimental designs [20] require 32 runs. Meanwhile, the number of regression coefficients to be estimate is 16. By taking into account the possibility that some of the main and interaction effects may be insignificant, a half replicate of the full 2^5 design was chosen as the experimental design. Furthermore, three central replicates were added to the experimental plan to estimate pure experimental error. The design of experimental matrix of acid activation of smectite and leaching yield of MgO is presented in Table 3. The response was expressed as mass% leaching yield of MgO calculated as $((C_0 - C)/C_0) \times 100$ where C_0 is the initial concentration of MgO and C is the final concentration of MgO.

To test the significance of the effects, an analysis of variance has been conducted at 95% confidence intervals. The results are shown in Table 4. Apart from the main and interaction effects, it is also possible to test the overall curvature generated by pure quadratic effects by means of the following statistics:

$$\mathrm{LOF}_{\mathrm{curv}} = \frac{m_0 F(\bar{y}_1 - \bar{y}_0)^2}{m_0 + F} \quad (2)$$

were $\bar{y}_0$ is the mean of central replicates and $\bar{y}_1$ is the mean of factorial experiments results. F is the number of experiments in factorial design and m_0 is the number of central replicates. As seen in Table 3, the analysis of variance detected a curvature effect.

Table 3
Experimental design and leaching yield of MgO

Run	X_1	X_2	X_3	X_4	X_5	MgO content (%)	
						Exp.	Pred
1	−1	1	−1	1	1	6.88	7.34
2	−1	−1	1	1	1	11.98	11.28
3	1	1	−1	1	−1	29.03	29.41
4	−1	−1	1	−1	−1	37.93	37.91
5	1	−1	1	1	−1	21.89	21.11
6	1	−1	1	−1	1	30.34	30.55
7	1	1	1	1	1	41.86	41.18
8	−1	1	−1	−1	−1	0.63	1.77
9	1	1	1	−1	−1	31.95	33.20
10	1	1	−1	−1	1	39.67	41.04
11	−1	1	1	−1	1	5.87	6.10
12	−1	1	1	1	−1	19.85	20.35
13	−1	−1	−1	1	−1	20.00	19.33
14	1	−1	−1	1	1	32.24	30.40
15	−1	−1	−1	−1	1	13.44	12.51
16	1	−1	−1	−1	−1	17.23	17.32
17	0	0	0	0	0	25.24	22.97
18	0	0	0	0	0	25.24	22.97
19	0	0	0	0	0	25.24	22.97

Table 4
Analysis of variance

Source of variance	Sum of squares	Degrees of freedom	Mean of squares	F-test	Probability > F
X_1	1018.09	1	1018.09	695.47	<0.0001
X_3	113.16	1	113.16	77.30	<0.0001
X_1X_2	516.77	1	516.77	353.01	<0.0001
X_1X_3	44.92	1	44.92	30.69	0.0005
X_1X_5	443.63	1	443.63	303.05	<0.0001
X_2X_4	65.33	1	65.33	44.63	0.0002
X_2X_5	29.89	1	29.89	20.42	0.0020
X_3X_4	47.92	1	47.92	32.74	0.0004
X_3X_5	137.53	1	137.53	93.95	<0.0001
Model	2417.24	9	268.58	183.47	<0.0001
Curvature	18.29	1	18.29	12.49	0.0077
Residual	11.71	8	1.46		
Lack of fit	11.71	6	1.95		
Total	2447.24	18			

According to the analysis of variance (Table 4) the F values for all regressions were higher. The large value of F indicates that most of the variation in the response can be explained by the regression model equation. The F value of 12.49 implies there is significant curvature (as measured by difference between the average of the center points and the average of the factorial points) in the design space.

Based on these results, the following model was obtained by regression analysis:

$$y_{\mathrm{Mg}} = 22.97 + 7.98X_1 + 2.66X_3 + 5.68X_1X_2 - 1.68X_1X_3 + 5.27X_1X_5 + 2.02X_2X_4 + 1.37X_2X_5 - 1.73X_3X_4 - 2.93X_3X_5 \quad (3)$$

The final equation in terms of the actual factors with the real word units follows:

Content of MgO = 124.43 − 1.46 × Temperature + 0.18 × Stirring speed + 0.38 × Temperature × Concentration − 0.001 × Temperature × Stirring speed + 0.53 × Temperature × Time + 0.90 × Concentration × Solid/liquid ratio + 0.91 × Concentration × Time − 0.008 × Stirring speed × Solid/liquid ratio − 0.019 × Stirring speed × Time.

The predicted values, using the model equations, compared with experimental result are shown in Table 3. The correlation coefficient of 0.995 indicates a good predictability of the model.

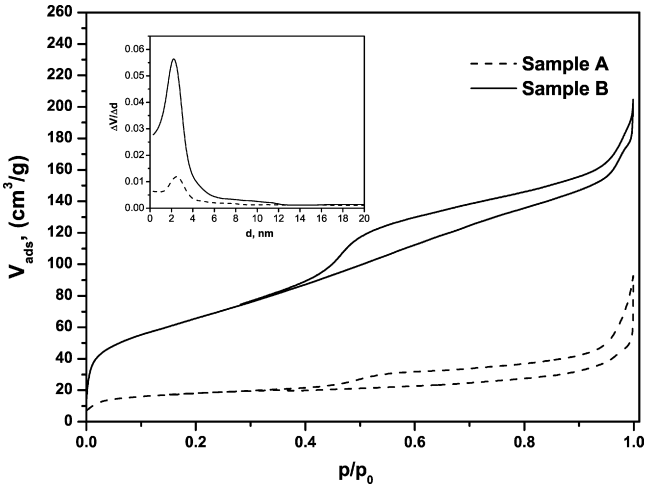

Fig. 1. N_2 adsorption–desorption isotherms of the natural (Sample A) and acid-activated (Sample B) smectite clays; inset is the corresponding pore size distribution curves.

As shown in Table 3, the highest leaching yield of MgO was obtained at 363 K, 6 M concentration, 600 rpm, solid-to-liquid ratio 1:6 and 3 h process duration (Sample B) while, the lowest leaching yield of MgO was obtained at 343 K, 6 M concentration, 300 rpm, solid-to-liquid ratio 1:3 and 1 h process duration.

The CEC of smectite sample activated under these conditions (Sample B) was slightly lower than the CEC of the starting smectite and amounted 74 meq/100 g. The reason for this behavior is, probably, dissolution of smectite flakes and deposition of amorphous silica [9].

The complete N_2 adsorption–desorption isotherms of the natural clay, sample A, and acid-activated smectite with the highest leaching yield of MgO, sample B, are shown in Fig. 1.

Both isotherms are reversible under a lower relative equilibrium pressure, but under a higher relative pressure they exhibit a hysteresis loop of the H3 type [27]. Such hysteresis loops exist in the slit-shaped pores or in the ink-bottle pores (pores with narrow necks and wide bodies). The values of the specific surface areas of the samples, S_{BET}, calculated by the BET method from nitrogen adsorption isotherms using data up to $p/p_o = 0.3$ are equal to 63 m^2/g for natural smectite clay (A), and 238 m^2/g, for the acid-activated sample (B). This indicates that acid activation increased the surface area of the smectite. This is possible due to the formation of active acid centers on the smectite flakes as a result of the structural modification during activation. However, the acid-activated smectite has increased the surface area [9]. The distribution of pores with widths from 2 to 50 nm was obtained by the calculation procedure given by Lippens et al. [25]. Derivatives of the cumulative pore volume curves with respect to slit width for both natural and acid-activated smectite clay are presented in Fig. 1. The pore size analysis shows that the sample A has mesopores with the most frequent size of 2.5 nm, while the acid-activated sample (Sample B) has mesopores with the most frequent size of 2.2 nm.The increasing peak amplitude of the sample B indicates that the pore volume increases with acid activation. These changes of the pore structure were the result of the removal of exchangeable cations and impurities

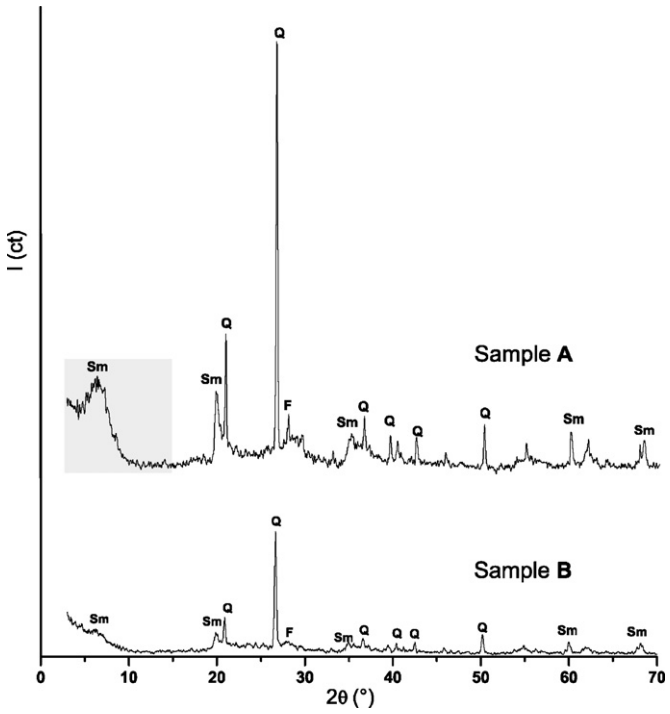

Fig. 2. X-ray diffraction patterns of natural (Sample A) and acid-activated (Sample B) smectite clays.

from the smectite by HCl. The large increase of the pore volume and the broadening of the pore size distribution observed in the activated smectite suggest that considerable structural changes and partial decomposition occurred in this sample.

XRD patterns used for mineralogical characterization of the natural clay (Sample A) are shown in Fig. 2.

The presence of smectite (Sm), illite (I), feldspar (F) and quartz (Q) is evident in the sample. The smectite phase in the starting material is confirmed by the XRD analyses of the oriented air-dried (AD), glycolated (EG) and calcined (723) samples (Fig. 3a).

The results of the XRD analysis for 0 0 1 spacing of the air-dried sample show reflection at 14.5 Å, which is characteristic of the presence of divalent cations. This indicates that the starting sodic smectite becomes progressively sodi-calcic during the process [26]. After ethylene glycol saturation the peak expands to 17.7 Å, indicating that the expandable layers of smectite type remain predominant, while calcinations at 723 K lead to a peak contraction to 10 Å. The XRD patterns from the Greene-Kelley test carried out on the starting sample, presented in Fig. 3b, show intermediate features, in particular the presence of two reflection lines at 8.9 and 17 Å. This indicates that the starting smectite transformed to another mineral of the smectite group characterized by a significant tetrahedral charge deficiency (beidellite) [26]. The relative amounts of the species were obtained from their corresponding peak areas. The results show that the montmorillonite/beidellite ratio in the raw smectite clay is 10/90. Thus, the smectite is predominantly beidellitic.

X-ray diffraction patterns of activated smectite clay (Sample B, Fig. 2) show the presence of peaks characteristic for smectite, illite, feldspar and quartz. In comparison with the diffraction

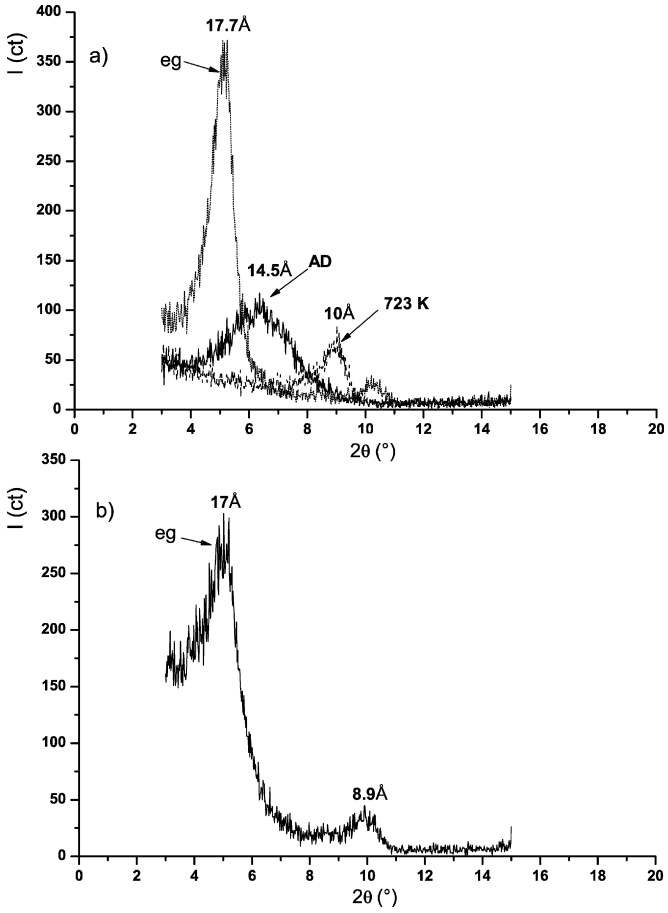

Fig. 3. XRD of natural smectite clay: (a) calcined, glycolated and oriented and (b) treated with LiCl at 473 K (Greene-Kelley test).

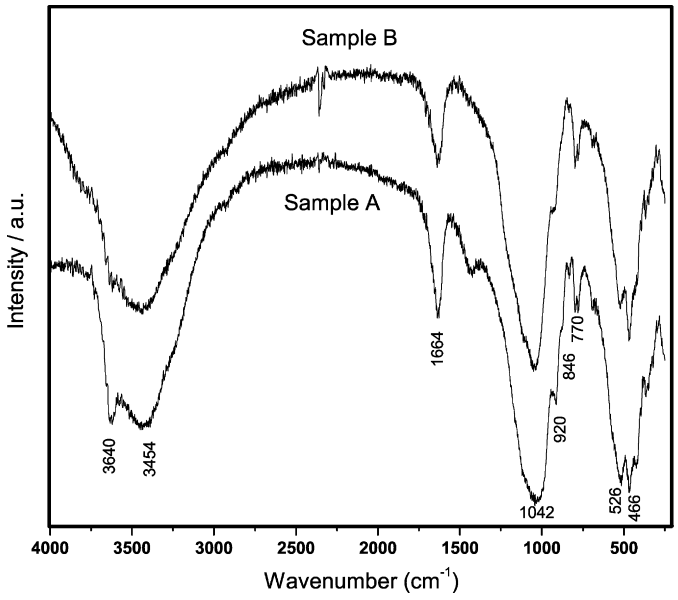

Fig. 4. IR spectra of natural (Sample A) and acid-activated (Sample B) smectite clay.

pattern of the starting material, the changes in the diffractogram of the activated material, shown by a decrease in the intensities of all reflections, indicate that the acid activation of smectitic clay leads to its partial decrystallization. As can be seen, the acid treatment affected mainly the smectitic phases.

The transmission spectra in the infrared region for the natural smectitic clay (Sample A) and the acid-activated smectitic clay (Sample B) are presented in Fig. 4.

As can be seen, the IR spectra confirmed the results of the XRD analysis, i.e., smectite was the dominant mineral phase. The IR band at 3640 cm^{-1} is attributed to stretching vibrations of the OH group associated with cations. The broad bands at 3454

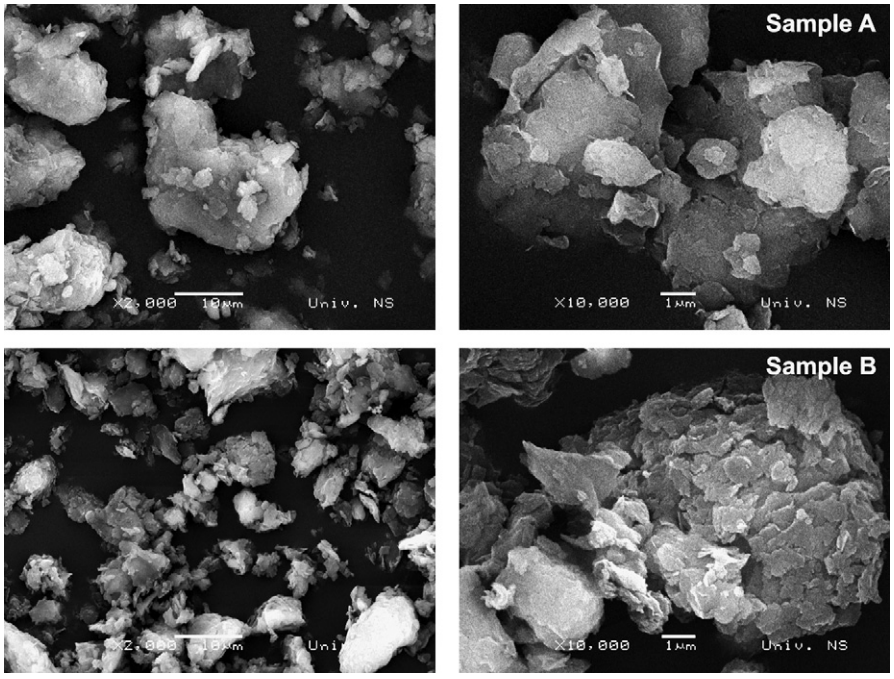

Fig. 5. SEM images of natural (Sample A) and acid-activated (Sample B) smectite clay.

and 1664 cm^{-1} show the stretching and deformation vibrations, respectively, for −OH groups of interlayer water molecules present in the clay. The bands at 1042 and 798 cm^{-1} are attributed to Si–O stretching vibrations. The band at 770 cm^{-1} corresponds to the beidellite species [28]. The dissolution of the octahedral sheets caused by acid treatment can be followed by an intensity decrease of the band corresponding to −OH bending vibration at 920 cm^{-1} (AlAlOH). The almost full disappearance of the band at 846 cm^{-1} assigned to AlMgOH points out to the occurrence of significant leaching of the Mg yield with acid activation. The bands at 526 and 466 cm^{-1} correspond to deformation vibrations of Si–O–Al and Si–O–Si, respectively. In the IR spectra of the acid-activated smectitic clay the intensities of the corresponding bands at 526 cm^{-1} (Si–O–Al), 466 cm^{-1} (Si–O–Si), 1042 cm^{-1} (Si–O), and 3454 cm^{-1} (adsorbed H_2O) were slightly reduced. The spectra show a significant decrease, almost a disappearance of the intensity at 3640 cm^{-1}, which indicates significant leaching of cations after the acid treatment.

The morphologies of the natural (Sample A) and acid-activated clay (Sample B) as observed by scanning electron microscope (SEM) are shown in Fig. 5.

SEM examination revealed a natural clay morphology of very fine, irregular, curved flakes and mats of coalesced flakes. In general, flakes seem to be anhedral, but it was difficult to determine their exact texture because of particle coalescence. A clear decrease in the particles size caused by acid activation is visible in Fig. 5. This sample predominantly consists of small aggregates of nanoparticles and exhibits a distinct porous structure.

4. Conclusion

In this study, statistically designed experiments were performed to investigate the recovery of Mg content from natural smectite clay from Serbia, with hydrochloric acid leaching. A first-order model which relates the MgO leaching yield to the process factors was obtained. The correlation coefficient of 0.995 indicates a good predictability of the model. On the basis of the model, the highest leaching yields of MgO were obtained at 363 K, 6 M HCl concentration, 600 rpm, solid-to-liquid ratio 1:6 and 3 h process conditions.

Chemical treatment of the natural smectite clay at the chosen conditions, by means of model, has developed the pore structure and adsorption properties of this clay. The sorption structural analysis shows that the acid-activated sample is characterized by a specific surface area of 238 m^2/g and that the slit-shaped mesopores of 2.2 nm are formed during the process of activation of smectite clay.

The results suggest that an adsorbent with optimal porosity and other adsorption properties can be produced by chemical treatment of the smectite clay.

Acknowledgments

This work was supported by the Ministry of Science and Environmental Protection of the Republic of Serbia (Projects number TR 6712B and ON 142019).

References

[1] D.F. Ovcharenko, Yu.I. Tarasevich, N.M. Radul, I.I. Marcin, N.S. Dyachenko, S.V. Nondarenko, Investigation of sorption on natural sorbents with different crystal structure, in: Natural Sorbent, Nauka, Moskva, 1967, p. 25.
[2] Sh. B. Battalova, Physico-chemical Basis of Production and Application of Catalysts and Adsorbents Based on Bentonite, Nauka, Kazakhskoi SSR, Alma-Ata, 1986, pp. 1–165.
[3] J.M. Adams, Synthetic organic chemistry using pillared, cation-exchanged and acid-treated montmorillonite catalysts—A review, Appl. Clay Sci. 2 (1987) 309.
[4] S.C. Kheok, E.E. Lim, Mechanism of palm oil bleaching by montmorillonite clay activated at various acid concentrations, J. Am. Oil Chem. Soc. 59 (1982) 129.
[5] D.A. Morgan, D.B. Shaw, T.C. Sidebottom, T.C. Soon, R.S. Taylor, The function of bleaching earth in the processing of palm, palm kernel and coconut oils, J. Am. Oil Chem. Soc. 62 (1985) 292.
[6] E. Srasra, F. Bergaya, H. van Damme, N.K. Arguib, Surface properties of an activated bentonite-decolorization of rapeseed oil, Appl. Clay Sci. 4 (1989) 411.
[7] D.R. Taylor, D.B. Jenkins, C.B. Ungermann, Bleaching with alternative layered minerals: A comparison with acid activated montmorillonite for bleaching soybean oil, J. Am. Oil Chem. Soc. 66 (1989) 334.
[8] C.N. Rhodes, D.R. Brown, Structural characterization and optimization of acid-treated montmorillonite and high-porosity silica supports for $ZnCl_2$ alkylation catalysts, J. R. Soc. Chem. Faraday Trans. 88 (1992) 2269.
[9] G.E. Christidis, P.W. Scott, A.C. Dunham, Acid activation and bleaching capacity of bentonite from the islands of Milos and Chios, Aegean, Greece, Appl. Clay Sci. 12 (1997) 329.
[10] G.E. Christidis, S. Kosiari, Decolorization of vegatable oils: A study of the mechanism of adsorption of β-carotene by an acid-activated bentonite from Cyprus, Clays Clay Miner. 51 (3) (2003) 327.
[11] N.N. Jovanovic, T.J. Janackovic, Pore structure and adsorption properties of an acid-activated bentonite, Appl. Clay Sci. 6 (1991) 59.
[12] B. Osthaus, Kinetic studies on montmorillonites and nontronite by the acid-dissolution technique, Clays Clay Miner. 4 (1956) 301.
[13] W.T. Granquist, G.G. Samner, Acid dissolution of a Texas bentonite, Clays Clay Miner. 6 (1959) 292.
[14] C.L. Thomas, J. Hickey, G. Stecker, Chemistry of clay cracking catalysts, Ind. Eng. Chem. 42 (1950) 866.
[15] T.H. Milliken, A.G. Oblad, G.A. Mills, Use of clays as petroleum cracking catalysis, Clays Clay Miner. 1 (1955) 314.
[16] I. Novak, B. Cicel, Dissolution of smectites in hydrochloric acid: II. Dissolution rate as a function of chrystallochemical composition, Clays Clay Miner. 26 (1978) 341.
[17] H. Kaviratna, T. Pinnavaia, Acid hydrolysis of octahedral Mg^{2+} sites in 2:1 layered silicates: an assessment of edge attack and gallery access mechanisms, Clays Clay Miner. 42 (1994) 717.
[18] A. Corma, A. Misfud, E. Sanz, Influence of the chemical composition and textural characteristics of palygorskite on the acid leaching of octahedral cations, Clays Clay Miner. 22 (1987) 225.
[19] R.W. Luce, R.W. Bartlett, G.A. Parks, Dissolution kinetics of magnesium silicates, Geochim. Cosmochim. Acta 36 (1972) 35.
[20] E. Şayan, M. Bayramoğlu, Statistical modeling of sulfuric acid leaching of TiO_2 from red mud, Hydrometallurgy 57 (2000) 181.
[21] O. Lacin, B. Bayrak, O. Korkut, E. Sayan, Modeling of adsorption and ultrasonic desorption of cadmium (II) and zinc (II) on local bentonite, J. Colloid Interface Sci. 292 (2005) 330.
[22] Ž. Lazić, Design of Experiments in Chemical Engineering, Wiley-VCH Verlag GmbH&Co. KGaA, Weinheim, 2004, p. 157.
[23] A. Gannouni, A. Bellagi, M. Nagane, Préparation d'une argile active pour la décoloration de l'huile d'olive, Ann. Chim.-Sci. Mat. 24 (1999) 407.
[24] S. Chegrouche, A. Bensmaili, Removal of Ga (III) from aqueous solution by adsorption on activated bentonite using a factorial design, Water Res. 36 (2002) 2898.

[25] B.C. Lippens, B.G. Linsen, J.H. De Boer, Studies on pore system in catalysts I. The Adsorption of nitrogen; apparatus and calculation, J. Catal. 3 (1964) 32.

[26] D. Guillaume, A. Neaman, M. Cathelineau, R. Mosser-Ruck, C. Peiffert, M. Abdelmoula, J. Dubessy, F. Villiéras, N. Michau, Experimental study of the transformation of smectite at 80 and 300 °C in the presence of Fe oxides, Clay Miner. 39 (1) (2004) 17.

[27] K. Sing, D. Everet, R. Haul, L. Moscou, R. Pierotti, J. Rouquerol, T. Siemieniewska, Reporting physisorption data for gas/solid systems with special reference to the determination of surface area and porosity, Pure Appl. Chem. 57 (1985) 603.

[28] E.L. Foletto, C. Volzone, L.M. Porto, Performance of an Argentinian acid-activated bentonite in the bleaching of soybean oil, Braz. J. Chem. Eng. 20 (2003).